

Implementing Riverine Biogeochemical Inputs in ECCO-Darwin: a Critical Step Forward for a Pioneering Data-Assimilative Global-Ocean Biogeochemistry Model

Raphaël Savelli^{1,2}, Dustin Carroll^{1,2}, Dimitris Menemenlis², Jonathan Lauderdale³, Clément Bertin², Stephanie Dutkiewicz^{3,4}, Manfredi Manizza⁵, Anthony Bloom², Karel Castro-Morales⁶, Charles E. Miller², Marc Simard², Kevin W. Bowman², and Hong Zhang²

¹Moss Landing Marine Laboratories, San José State University, Moss Landing, CA, USA

²Jet Propulsion Laboratory, California Institute of Technology, Pasadena, CA, USA

³Department of Earth, Atmospheric and Planetary Sciences, Massachusetts Institute of Technology, Cambridge, Massachusetts, USA

⁴Center for Global Change Science, Massachusetts Institute of Technology, Cambridge, Massachusetts, USA

⁵National Institute of Oceanography and Applied Geophysics - OGS, Sgonico, Italy

⁶Deutscher Wetterdienst, Climate and Environment, Offenbach, Germany

Correspondence: Raphaël Savelli (raphael.savelli@sjsu.edu)

Supporting Information

Text S1: Additional River Inputs Evaluation

Along with 39,687 km³ yr⁻¹ of riverine freshwater, net inputs of 551.9 Tg C yr⁻¹, 35 Tg N yr⁻¹, and 139.7 Tg Si yr⁻¹ were routed into the global ocean in ALL_{run} (Figure S1). The Arctic Ocean region (Figure S1, ARCT) received 5,138 km³ yr⁻¹ of freshwater from rivers in Baseline, which is roughly 13% of global freshwater discharge. In ALL_{run}, freshwater discharge was supplemented with 22.6 and 56.8 Tg C yr⁻¹ of t_{DOC} and t_{DIC} input, respectively (Figure S1). The regional input of t_{DIC} and t_{DOC} into ARCT represented 15% and 13% of their associated global input, respectively. ARCT also received 2.5 Tg N yr⁻¹ as t_{DON} (56%) and t_{DIN} (44%) in ALL_{run}; t_{DSi} input was 12.6 Tg Si yr⁻¹ (Figure S1). Inputs were primarily from the Ob, Yenisey, Lena, and Mackenzie Rivers (Figure S1 and Table S1). The Tropical Atlantic (Figure S1, TROP-ATL) received 36% of global freshwater discharge (14,228 km³ yr⁻¹) and 35% of the global t_{DOC} input from rivers (67.2 Tg C yr⁻¹). Combined with t_{DIC}, the net carbon input was 145.3 Tg C yr⁻¹ (Figure S1). Roughly 30% of global dissolved nitrogen and silica inputs were delivered to TROP-ATL, with inputs dominated by the Amazon River (Figure S1 and Table S1). In Baseline, freshwater discharge into SE-ASIA was 7,841 km³ yr⁻¹, roughly 20% of global discharge. In ALL_{run}, SE-ASIA received 38% of dissolved carbon input (globally 207.39 Tg C yr⁻¹). 81% of dissolved carbon input into SE-ASIA was inorganic, representing 42% of the global t_{DIC} input (Figure S1). SE-ASIA also received 45% (10.6 Tg N yr⁻¹) of the global t_{DIN} input (Figure S1), with 41.5 Tg Si yr⁻¹ (30% of global t_{DSi} input) (Figure S1). Nutrient inputs into SE-ASIA were dominated by high t_{DIC} and t_{DIN} from the Ganges and Yangtze Rivers (Figure S1 and Table S1). The Yangtze river contributed 12% of

t_{DIC} input, globally (Figure S1 and Table S1). Taken together, the Yangtze and Ganges Rivers delivered 20% of the global t_{DIN} input (Figure S1 and Table S1).

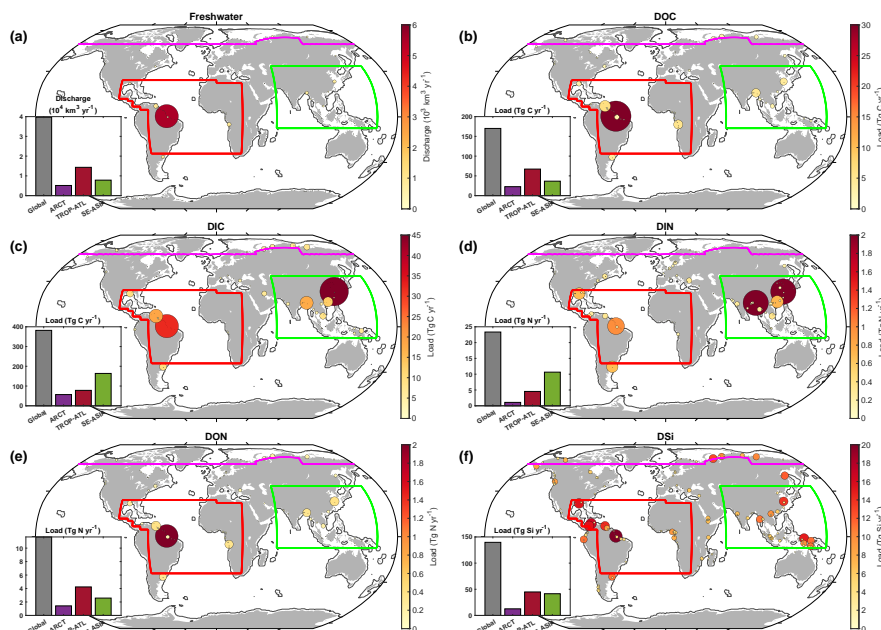


Figure S1. Riverine freshwater discharge and biogeochemical inputs resulting from the association of Global NEWS 2 and JRA55-do on the LLC90 grid. Domain-scale freshwater discharge and load are relative to the respective domain area. The insets show corresponding year-2000 discharge/load for various regions. The size of the circles represents the magnitude of loads. Colored boundary lines correspond to domains used for regional analysis of the Arctic Ocean (ARCT, violet line), the Tropical Atlantic (TROP-ATL, red line), and Southeast Asia (SE-ASIA, green line). The black line delineates the coastal ocean from the open ocean, which is set by the furthest point from the coastline of either a 300-km distance or the 1000-m isobath. Only rivers with annual discharge over $10 \text{ km}^3 \text{ yr}^{-1}$ are shown.

Table S1. Freshwater discharge and inputs for single-river experiments.

River	Freshwater					
	Discharge (km ³ yr ⁻¹)	t_{DIC} (Tg C yr ⁻¹)	t_{DOC} (Tg C yr ⁻¹)	t_{DIN} (Tg N yr ⁻¹)	t_{DON} (Tg N yr ⁻¹)	t_{DSi} (Tg Si yr ⁻¹)
Amazon	6834.6	32.2	30.7	1	1.9	20.7
Nile	68	1.1	0.3	0.1	0.02	0.2
Congo	1116.2	0.8	5.4	0.2	0.3	2.1
Mississippi	622.5	9.5	3	0.7	0.2	1.5
Ob	453.5	6.75	2.6	0.1	0.15	1.3
Paraná	942.1	9.8	3.8	0.7	0.3	1.1
Yenisey	652.3	6.8	3	0.1	0.2	1
Lena	554.8	8.2	2.4	0.1	0.2	1
Niger	211.2	>0.01	0.9	0.1	0.1	0.9
Yangtze	990.9	45.9	4.2	2.1	0.4	1.4
Amur	384.4	0.01	1.85	0.2	0.1	1.2
Mackenzie	301.4	4	1.8	0.03	0.1	0.7
Ganges	976.4	18.01	5	2.2	0.3	2.8
Zambezi	103.65	>0.01	0.5	0.02	0.03	0.6
Indus	76.3	0.35	0.4	0.1	0.04	0.02

Table S2. Arctic rivers inputs in the present study and from the ArcticGRO monitoring network (Holmes et al., 2012; Tank et al., 2023).

	t_{ALK} (Tg C yr ⁻¹)		t_{DOC} (Tg C yr ⁻¹)		t_{DIN} (Tg N yr ⁻¹)		t_{DSi} (Tg Si yr ⁻¹)	
	This study	ArcticGRO	This study	ArcticGRO	This study	ArcticGRO	This study	ArcticGRO
Ob	6.6	4.1	2.6	4.9	0.1	0.1	1.3	1.9
Yenisey	6.7	5	3	5	0.1	0.05	1	2.1
Mackenzie	3.9	3.7	1.8	1.6	0.03	0.02	0.7	0.5
Lena	8	6.5	2.4	9.8	0.1	0.08	1	2.5
Kolyma	0.07	0.4	0.6	1.1	0.01	0.01	0.2	0.3
Yukon	0.9	2.6	0.4	2.3	0.01	0.03	0.3	0.8

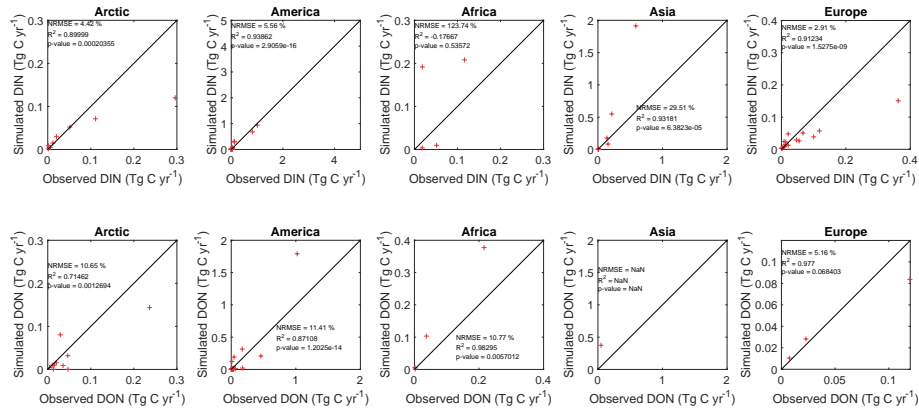


Figure S2. Regional comparisons of observed and simulated t_{DIN} and t_{DON} in Global NEWS 2 (Mayorga et al., 2010). The normalized root-mean-square error corresponds to the root-mean-square error divided by the range between the maximal and minimal values in observations.

20 Text S2: Additional Sensitivity Experiments

We ran additional sensitivity experiments using all riverine inputs (Table S3, ALL_{run}) for each of the top-15 global rivers (i.e., isolating the impact of individual rivers) in terms of watersheds extent (Mayorga et al., 2010). Input-driven CO₂ outgassing was dominated by the input of t_{DOC} in ARCT, with 50% of the associated CO₂ outgassing due to the Ob, Yenisey, Lena, and Mackenzie Rivers (Table S3). The Amazon River drove 70% of input-driven CO₂ outgassing in TROP-ATL (Table S3).
 25 Notably, the Amazon River was responsible for 65% of the NPP increase, driven by inputs in this region (Table S3). The Ganges River (58%), combined with the Indus and Yangtze Rivers, are responsible for 77% of CO₂ uptake in SE-ASIA (Table S3). Nitrogen and silica inputs from the Ganges and Yangtze rivers drive roughly 40% of the NPP increase in SE-ASIA (Table S3). The top 15 rivers drove a CO₂ ocean outgassing of 9.5 Tg C yr⁻¹ and contributed up to 31% of the global ocean outgassing driven by world rivers (Table S3). In addition, the top 15 rivers were responsible for 50% of the increase of NPP driven by
 30 global inputs (302.4 Tg C yr⁻¹, Table S3).

Table S3. Contribution of the global top 15 rivers to changes in air-sea CO₂ flux and NPP. Positive values represent CO₂ outgassing driven by the corresponding river; negative values are uptake. The respective river contribution is estimated from the difference between Baseline and a modified ALL_{run}, where only the corresponding river was included. The top 15 rivers were selected based on watershed area.

Rank	River	$\Delta \text{CO}_2 \text{ Flux}$	ΔNPP
		(Tg C yr ⁻¹)	(Tg C yr ⁻¹)
1	Amazon	+14.3	+113.6
2	Nile	+0.3	-0.1
3	Congo	+1.3	+12.4
4	Mississippi	-1.3	+26.4
5	Ob	+2	+2.2
6	Paraná	+0.5	+13.5
7	Yenisey	+2.6	+1.5
8	Lena	+2.8	+1.1
9	Niger	-0.1	+3
10	Yangtze	-3	+57.3
11	Amur	+0.7	+1.7
12	Mackenzie	+1.7	+0.6
13	Ganges	-11.7	+64.5
14	Zambezi	+0.1	+1
15	Indus	-0.7	+3.7
Total		+9.5	+302.4

Text S3: Suggested Additional Land-to-Ocean Model Improvements

In this section, we elaborate on additional necessary model improvements to better quantify the role of inputs on air-sea CO₂ fluxes and ocean biogeochemistry.

We note that we only considered surface-ocean freshwater discharge, which represents roughly 39,000 km³ yr⁻¹ delivered to the ocean. However, a significant fraction of freshwater discharge to the ocean (10%) originates from groundwater discharge (Taniguchi et al., 2002). While the net impact on the open-ocean carbon cycle is small, this discharge volume and associated biogeochemical elements can substantially impact the coastal ocean through eutrophication (Luijendijk et al., 2020). Groundwater discharge inputs the equivalent of 23%, 7.5%, and 8% of riverine DIC, DIN, and DSi, respectively (Luijendijk et al., 2020). In addition to groundwater discharge, subglacial discharge from marine-terminating glaciers, particularly in Greenland and the West Antarctic Peninsula, would need to be fluxed at subsurface depths and take subglacial plume entrainment into account (Carroll et al., 2016; Slater and Straneo, 2022). In addition to the physical impact of freshwater inputs on the ocean,

subglacial upwelling of nutrients (Hopwood et al., 2018) and meltwater from ice sheets and icebergs (Hopwood et al., 2020) is a significant source of reactive iron that can support coastal high-latitude marine ecosystems (Hawkings et al., 2014; Hopwood et al., 2020). While their present contribution to global-ocean carbon cycling remains unknown, groundwater and subglacial
45 discharge are expected to be altered by climate change (changes in storm and cyclone frequency and intensity, rising land and ocean temperatures, increased cryosphere melt, changes in ocean chemistry and coastal erosion) and human activities such as groundwater extraction (Richardson et al., 2024).

Moreover, heat from river discharge is omitted in our simulations. In the Arctic Ocean, where sea-ice cover is negatively correlated with heat from river discharge, the addition of point-source freshwater discharge should be supplemented with
50 realistic water temperature to accurately represent sea-ice dynamics in response to riverine heat fluxes (Manak and Mysak, 1989; Whitefield et al., 2015; Park et al., 2020; Dong et al., 2022). Additionally, chromophoric dissolved organic matter (CDOM) absorbs heat and thus can increase thermal stratification near the surface ocean (Morris et al., 1995; Laurion et al., 1997; Caplanne and Laurion, 2008). In the Chukchi Sea, Hill (2008) associated the 40%-increase of energy absorption by the mixed layer in spring to the presence of ice algae. The heat absorption by dissolved organic matter may cause an amplification
55 of Arctic Ocean warming if the delivered amount of terrestrial material and DOC increases in the future.

Finally, we scale the annual carbon or nutrient concentration from Global NEWS 2 with daily freshwater fluxes from JRA55-do to obtain time-varying, point-source inputs. Consequently, the seasonal cycle of biogeochemical fluxes tracks the seasonality of freshwater discharge in JRA55-do — which is a simplified first-order approximation. First, we acknowledge that the JRA55-do seasonal cycle of freshwater discharge can be inaccurate in specific regions (e.g., Arctic regions), and we also assume a direct
60 relationship between carbon/nutrient concentrations and freshwater discharge (Suzuki et al., 2018; Tsujino et al., 2018; Feng et al., 2021). Second, we compute carbon/nutrient concentrations based on annual inputs from Global NEWS 2 and assume these values are constant throughout the year. Global observations have shown that the relationship between carbon/nutrient fluxes and freshwater discharge is not always valid, with concentrations changing on a sub-annual basis (Jordan et al., 1991; Le Fouest et al., 2013; Holmes et al., 2012; Bittar et al., 2016; Shogren et al., 2021; Kamjunke et al., 2021). Processes such
65 as changes in land use, human inputs, sewage leaks, enhanced permafrost thaw, decomposition, or changes in basin hydrology can seasonally alter the concentration of biogeochemical substances without inducing changes in freshwater discharge — to account for these deficiencies, a land-surface model accounting for such processes, the Bayesian CARbon DATA-MODEl fraMework (CARDAMOM) (Bloom et al., 2020), is currently being coupled with ECCO-Darwin.

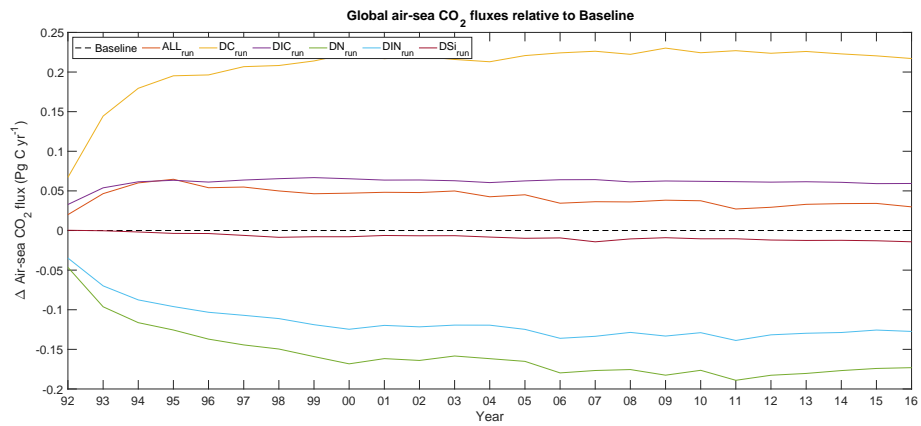


Figure S3. Globally integrated air-sea CO₂ flux time series relative to ECCO-Darwin Baseline. Air-sea CO₂ fluxes are annual means from January 1992 to December 2019. Positive values represent CO₂ outgassing; negative values represent uptake.

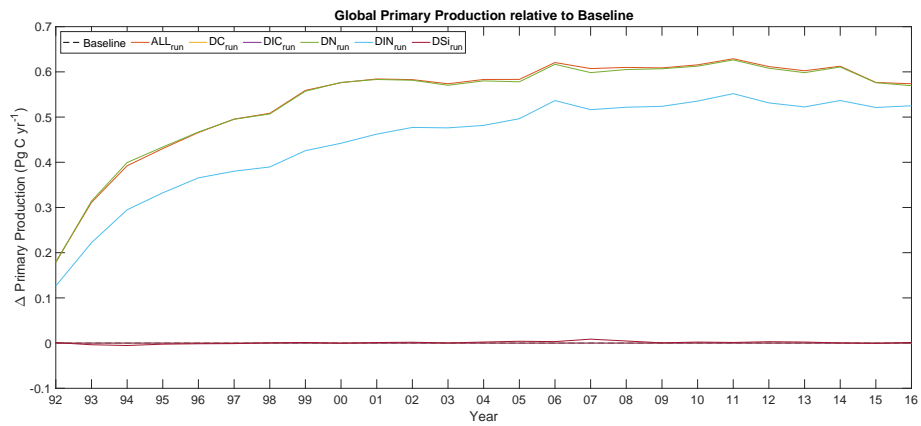


Figure S4. Globally integrated net primary production time series relative to ECCO-Darwin Baseline. Primary production is annual means from January 1992 to December 2019.

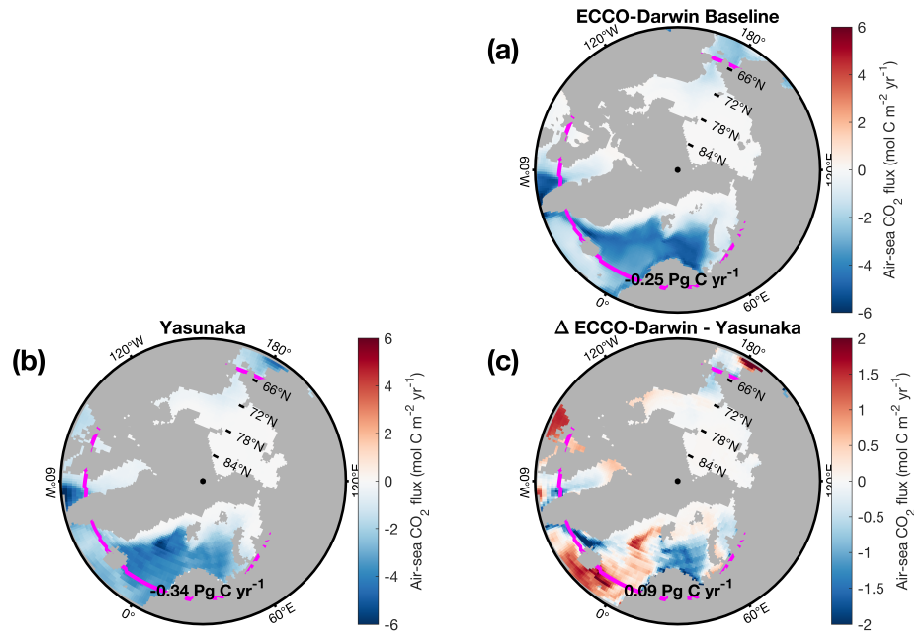


Figure S5. Climatological global-ocean air-sea CO₂ flux for (a) ECCO-Darwin Baseline and (b) Yasunaka data-based product (Yasunaka et al., 2023). Panel (c) corresponds to the difference between ECCO-Darwin Baseline and Yasunaka data-based product. Positive values represent CO₂ outgassing (red colors); negative values represent uptake (blue colors). All fields shown are time means from January 1997 to December 2014. Colored boundary lines correspond to the domain used for regional analysis of the Arctic Ocean (ARCT, violet line). The Yasunaka data-based product was interpolated on the LLC90 grid. Net air-sea CO₂ flux are integrated for the entire domain (Latitude > 60.5°).

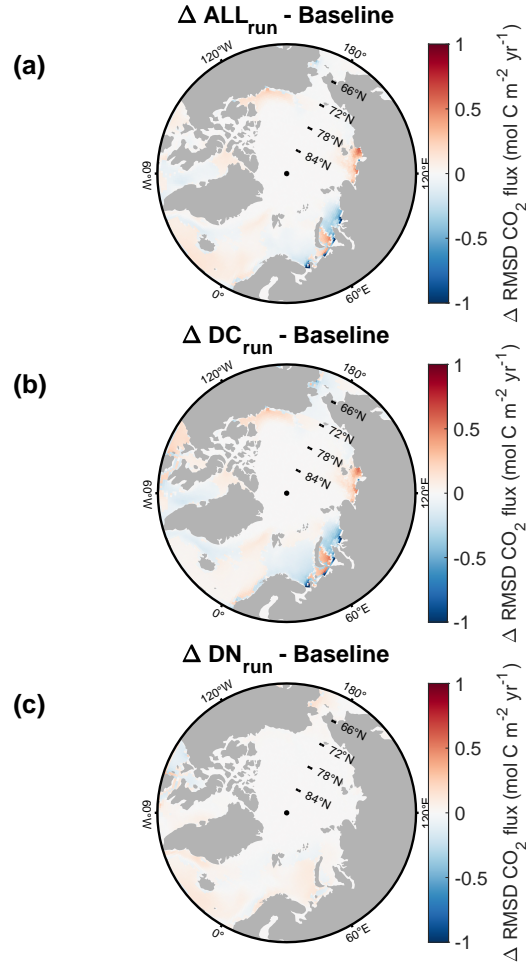


Figure S6. Change in root-mean-square deviation (RMSD) of air-sea CO_2 flux between ECCO-Darwin Baseline and (a) ALL_{run} , (b) DC_{run} , and (c) DN_{run} compared to the Yasunaka data-based product (Yasunaka et al., 2023). Positive values represent an increase of the deviation (red colors); negative values show a smaller deviation (blue colors). All fields shown are time means from January 1997 to December 2014.

References

- 70 Bittar, T. B., Berger, S. A., Birsá, L. M., Walters, T. L., Thompson, M. E., Spencer, R. G., Mann, E. L., Stubbins, A., Frischer, M. E., and Brandes, J. A.: Seasonal dynamics of dissolved, particulate and microbial components of a tidal saltmarsh-dominated estuary under contrasting levels of freshwater discharge, *Estuarine, Coastal and Shelf Science*, 182, 72–85, <https://doi.org/https://doi.org/10.1016/j.ecss.2016.08.046>, 2016.
- Bloom, A. A., Bowman, K. W., Liu, J., Konings, A. G., Worden, J. R., Parazoo, N. C., Meyer, V., Reager, J. T., Worden, H. M., Jiang, Z.,
75 et al.: Lagged effects regulate the inter-annual variability of the tropical carbon balance, *Biogeosciences*, 17, 6393–6422, 2020.
- Caplanne, S. and Laurion, I.: Effect of chromophoric dissolved organic matter on epilimnetic stratification in lakes, *Aquatic Sciences*, 70, 123–133, 2008.
- Carroll, D., Sutherland, D. A., Hudson, B., Moon, T., Catania, G. A., Shroyer, E. L., Nash, J. D., Bartholomäus, T. C., Felikson, D., Stearns, L. A., et al.: The impact of glacier geometry on meltwater plume structure and submarine melt in Greenland fjords, *Geophysical Research*
80 *Letters*, 43, 9739–9748, 2016.
- Dong, J., Shi, X., Gong, X., Astakhov, A. S., Hu, L., Liu, X., Yang, G., Wang, Y., Vasilenko, Y., Qiao, S., et al.: Enhanced Arctic sea ice melting controlled by larger heat discharge of mid-Holocene rivers, *Nature Communications*, 13, 5368, 2022.
- Feng, Y., Menemenlis, D., Xue, H., Zhang, H., Carroll, D., Du, Y., and Wu, H.: Improved representation of river runoff in Estimating the Circulation and Climate of the Ocean Version 4 (ECCOV4) simulations: implementation, evaluation, and impacts to coastal plume regions, *Geoscientific Model Development*, 14, 1801–1819, 2021.
85
- Hawkings, J. R., Wadham, J. L., Tranter, M., Raiswell, R., Benning, L. G., Statham, P. J., Tedstone, A., Nienow, P., Lee, K., and Telling, J.: Ice sheets as a significant source of highly reactive nanoparticulate iron to the oceans, *Nature communications*, 5, 3929, 2014.
- Hill, V. J.: Impacts of chromophoric dissolved organic material on surface ocean heating in the Chukchi Sea, *Journal of Geophysical Research: Oceans*, 113, <https://doi.org/https://doi.org/10.1029/2007JC004119>, 2008.
- 90 Holmes, R. M., McClelland, J. W., Peterson, B. J., Tank, S. E., Bulygina, E., Eglinton, T. I., Gordeev, V. V., Gurtovaya, T. Y., Raymond, P. A., Repeta, D. J., et al.: Seasonal and annual fluxes of nutrients and organic matter from large rivers to the Arctic Ocean and surrounding seas, *Estuaries and Coasts*, 35, 369–382, 2012.
- Hopwood, M. J., Carroll, D., Browning, T. J., Meire, L., Mortensen, J., Krisch, S., and Achterberg, E. P.: Non-linear response of summertime marine productivity to increased meltwater discharge around Greenland, *Nature Communications*, 9, 3256, 2018.
- 95 Hopwood, M. J., Carroll, D., Dunse, T., Hodson, A., Holding, J. M., Iriarte, J. L., Ribeiro, S., Achterberg, E. P., Cantoni, C., Carlson, D. F., Chierici, M., Clarke, J. S., Cozzi, S., Fransson, A., Juul-Pedersen, T., Winding, M. H. S., and Meire, L.: Review article: How does glacier discharge affect marine biogeochemistry and primary production in the Arctic?, *The Cryosphere*, 14, 1347–1383, <https://doi.org/10.5194/tc-14-1347-2020>, 2020.
- Jordan, T. E., Correll, D. L., Miklas, J. J., and Weller, D. E.: Long-term trends in estuarine nutrients and chlorophyll, and short-term effects
100 of variation in watershed discharge, *Marine Ecology Progress Series*, 1991.
- Kamjunke, N., Rode, M., Baborowski, M., Kunz, J. V., Zehner, J., Borchardt, D., and Weitere, M.: High irradiation and low discharge promote the dominant role of phytoplankton in riverine nutrient dynamics, *Limnology and Oceanography*, 66, 2648–2660, <https://doi.org/https://doi.org/10.1002/lno.11778>, 2021.
- Laurion, I., Vincent, W. F., and Lean, D. R.: Underwater ultraviolet radiation: development of spectral models for northern high latitude
105 lakes, *Photochemistry and Photobiology*, 65, 107–114, 1997.

- Le Fouest, V., Babin, M., and Tremblay, J.-É.: The fate of riverine nutrients on Arctic shelves, *Biogeosciences*, 10, 3661–3677, 2013.
- Luijendijk, E., Gleeson, T., and Moosdorf, N.: Fresh groundwater discharge insignificant for the world’s oceans but important for coastal ecosystems, *Nature communications*, 11, 1260, 2020.
- Manak, D. K. and Mysak, L. A.: On the relationship between arctic sea-ice anomalies and fluctuations in Northern Canadian air temperature and river discharge, *Atmosphere-Ocean*, 27, 682–691, 1989.
- Mayorga, E., Seitzinger, S. P., Harrison, J. A., Dumont, E., Beusen, A. H., Bouwman, A., Fekete, B. M., Kroeze, C., and Van Drecht, G.: Global nutrient export from WaterSheds 2 (NEWS 2): model development and implementation, *Environmental Modelling & Software*, 25, 837–853, 2010.
- Morris, D. P., Zagarese, H., Williamson, C. E., Balseiro, E. G., Hargreaves, B. R., Modenutti, B., Moeller, R., and Queimalinos, C.: The attenuation of solar UV radiation in lakes and the role of dissolved organic carbon, *Limnology and Oceanography*, 40, 1381–1391, 1995.
- 115 Park, H., Watanabe, E., Kim, Y., Polyakov, I., Oshima, K., Zhang, X., Kimball, J. S., and Yang, D.: Increasing riverine heat influx triggers Arctic sea ice decline and oceanic and atmospheric warming, *Science advances*, 6, eabc4699, 2020.
- Richardson, C., Davis, K., Ruiz-González, C., Guimond, J., Michael, H., Paldor, A., Moosdorf, N., and Paytan, A.: The impacts of climate change on coastal groundwater, *Nature Reviews Earth & Environment*, pp. 1–20, 2024.
- 120 Shogren, A. J., Zarnetske, J. P., Abbott, B. W., Iannucci, F., Medvedeff, A., Cairns, S., Duda, M. J., and Bowden, W. B.: Arctic concentration–discharge relationships for dissolved organic carbon and nitrate vary with landscape and season, *Limnology and Oceanography*, 66, S197–S215, <https://doi.org/https://doi.org/10.1002/lno.11682>, 2021.
- Slater, D. and Straneo, F.: Submarine melting of glaciers in Greenland amplified by atmospheric warming, *Nature Geoscience*, 15, 794–799, 2022.
- 125 Suzuki, T., Yamazaki, D., Tsujino, H., Komuro, Y., Nakano, H., and Urakawa, S.: A dataset of continental river discharge based on JRA-55 for use in a global ocean circulation model, *Journal of oceanography*, 74, 421–429, 2018.
- Taniguchi, M., Burnett, W. C., Cable, J. E., and Turner, J. V.: Investigation of submarine groundwater discharge, *Hydrological Processes*, 16, 2115–2129, 2002.
- Tank, S. E., McClelland, J. W., Spencer, R. G., Shiklomanov, A. I., Suslova, A., Moatar, F., Amon, R. M., Cooper, L. W., Elias, G., Gordeev, V. V., et al.: Recent trends in the chemistry of major northern rivers signal widespread Arctic change, *Nature Geoscience*, 16, 789–796, 2023.
- 130 Tsujino, H., Urakawa, S., Nakano, H., Small, R. J., Kim, W. M., Yeager, S. G., Danabasoglu, G., Suzuki, T., Bamber, J. L., Bentsen, M., et al.: JRA-55 based surface dataset for driving ocean–sea-ice models (JRA55-do), *Ocean Modelling*, 130, 79–139, 2018.
- Whitefield, J., Winsor, P., McClelland, J., and Menemenlis, D.: A new river discharge and river temperature climatology data set for the pan-Arctic region, *Ocean Modelling*, 88, 1–15, 2015.
- 135 Yasunaka, S., Manizza, M., Terhaar, J., Olsen, A., Yamaguchi, R., Landschützer, P., Watanabe, E., Carroll, D., Adiwira, H., Müller, J. D., and Hauck, J.: An Assessment of CO₂ Uptake in the Arctic Ocean From 1985 to 2018, *Global Biogeochemical Cycles*, 37, e2023GB007806, <https://doi.org/https://doi.org/10.1029/2023GB007806>, e2023GB007806 2023GB007806, 2023.